POST-IMBRIAN GLOBAL LUNAR TECTONISM: EVIDENCE FOR AN INITIALLY TOTALLY MOLTEN MOON

ALAN B. BINDER
Institut für Mineralogie, Universität Münster, West Germany

(Received 8 October 1981)

Abstract. Evaluation of all reasonable sources of stress in the lunar crust indicates that compressional thermoelastic stresses are the only ones which have been tectonically significant on the global scale during the last 3.5×10^9 yr of lunar history – i.e., the post-Imbrian. However, the thermoelastic stresses calculated for lunar models which have accretional heating profiles at the beginning of lunar history; i.e., a molten zone only a few hundred kilometers deep and a cool deep interior, are less than 1 kbar in the crust. Such stresses are lower than the more than 1 to 7 kbar needed to initiate thrust faulting in the outer crust according to Anderson's theory of thrust faulting. Thus such accretional models predict that no significant global thrust faulting has occurred during the post-Imbrian and that the crust should currently be seismically quiet on the global scale.

In contrast, the compressional thermoelastic stresses generated in a Moon which was initially totally molten, as is the case if the Moon formed by fission, are up to 3.5 kbar in the outer few km of the crust at present. These stresses are well within the range needed to cause thrust faulting in the outer 4 km of the crust. According to this model there should be modest scale (10 km), young ($\leqslant 0.5$ to 1×10^9 yr old) thrust fault scarps in the highlands.

Photoselenological investigations confirm that scarps with the expected age and geometric characteristics are found in the highlands. Thus the currently available photoselenological data support the stress model derived for an initially totally molten Moon, but not one which was molten only in the outer few hundreds of km.

1. Introduction

The initial thermal state of the Moon was a decisive factor in determining the course of its early development and later evolution. If the Moon was initially totally molten, as is expected if it formed by fission (e.g., Binder, 1974, 1978, 1980) or if it underwent rapid ($\lesssim 10^7$ yr) melting due to short lived radioactive elements (e.g., Runcorn, 1977), many of its compositional and physical characteristics would be diagnostically different from those it would have if it formed by accretion and only the outer few hundreds of kilometers were initially molten (e.g., Solomon and Chaiken, 1976; Solomon and Longhi, 1977; Longhi, 1977). As discussed in this paper, the post-Imbrian, global tectonism of the Moon is highly dependent on its initial thermal state and may be used to distinguish between the two possibilities indicated above.

2. Post-Imbrian Global Stresses

As discussed shortly, the two contrasting thermoelastic stress models (Solomon and Chaiken, 1976; Binder and Lange, 1980) used as a basis for this study show that the crust of the Moon began to undergo a phase of compressional stress of ever increasing

The Moon and the Planets **26** (1982) 117–133. 0165–0807/82/0262–0117$02.55.

magnitude about 3.5×10^9 yr ago. This phase, which covers the entire post-Imbrian (as well as the last one or two hundred million years of the Imbrian), defines the period of interest of this study.

Exogenetic tectonism has been important only on the local scale during the post-Imbrian since post-Imbrian impact craters are all smaller than about 100 km. Endogenetic tectonism related to the read-justment of the crust in response to the mare basalt loads during the post-Imbrian is limited to the maria (e.g., Solomon and Head, 1979) and hence is only of regional importance. Even though there is observational and theoretical evidence which indicates that solid state convection has never been active in the Moon (Binder and Lange, 1980), the lunar lithosphere has been sufficiently thick during the post-Imbrian so that any convection associated stresses most probably could not have affected the upper crust, even if the mantle did convect. The lithosphere thickness is found to have been about 50 km just before 3.5×10^9 yr ago and about 200 km at the present (Comer *et al.*, 1979; Binder and Lange, 1980; see curve T_c in their Figure 6). Hence, the only likely global stresses present during the post-Imbrian are those associated with the decreases in the tidal bulge and the oblateness of the Moon as it moved away from the Earth and the thermoelastic stresses. It is shown in the following that only the thermoelastic stresses have been important.

2.1. Tidal and Rotational Stresses

As shown by Jeffreys (1962), the tidal effect due to the Earth's gravity and the centrifugal effect due to the Moon's rotation (locked with respect to the Earth) combine to distort the Moon into a triaxial ellipsoid. The lengths of the a (Earth directed), b (tangential to orbit), and c (perpendicular to orbit) axes are given by Jeffreys as

$$a = r(1 + 35Mr^3/12mD_e^3), \tag{1}$$

$$b = r(1 - 10Mr^3/12mD_e^3), \tag{2}$$

$$c = r(1 - 25Mr^3/12mD_e^3), \tag{3}$$

where r is the mean radius of the Moon (1.738×10^8 cm), m is the mass of the Moon (7.35×10^{25} gm), M is the mass of the Earth (5.98×10^{27} gm), and D_e is the mean Earth–Moon distance (currently 3.844×10^{10} cm). Since a, b, and c are proportional to D_e^{-3}, any change in D_e results in a change in the figure of the Moon and hence to the formation of stresses in the lunar crust. From the development of Melosh (1977, 1980), the maximum stress (σ_t) produced in the crust if the Moon moved from some D_e to infinity is given by

$$\sigma_t \leqslant \tfrac{4}{5}\mu f \tag{4}$$

for a hydrostatic Moon with a thin lithosphere, and

$$\sigma_t \leqslant \tfrac{8}{25}\mu h f \tag{5}$$

for an elastic, but incompressible Moon (i.e., the two limiting cases of interest), where μ is the rigidity of the Moon (6×10^{11} dynes cm^{-2}), h is the second Love number, and f is $(a - c)/a$ using (1) and (3). The second Love number

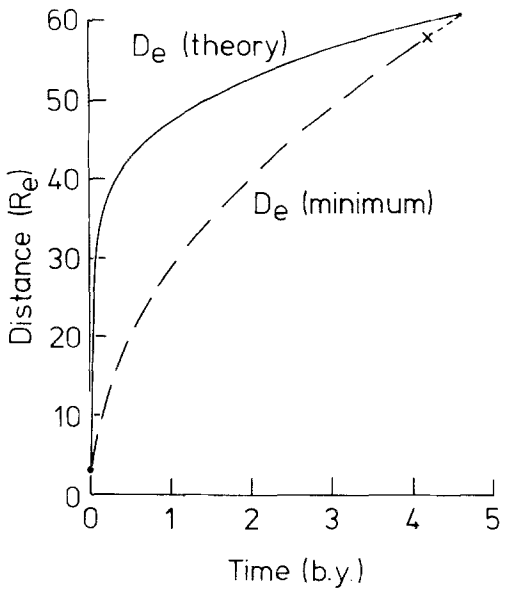

Fig. 1. Earth–Moon distance as a function of time. At $t = 0$ the Moon is assumed to have been at 3 Earth radii (R_e) from the Earth. Curve D_e (theory) is derived from the theoretical expression in which $D_e \propto t^{2/13}$ and most probably is a good, average approximation to the true D_e. The dashed curve, D_e (minimum), which is tied to point X derived from fossil data, is a conservative lower limit for D_e which is assumed to vary with $t^{1/2}$.

$$h = \tfrac{5}{2}(1 + 19\mu/2g\rho r)^{-1}, \tag{6}$$

where g is the lunar gravity (162.3 cm s^{-2}) and ρ is the density of the Moon (3.34 g cm^{-3}).

Given these equations, one can obtain the tidal and rotational related stresses caused in the crust as the Moon moved away from the Earth, assuming we know the evolutional history of the Lunar orbit. Figure 1 gives D_e as a function of time assuming that the dissipation of tidal energy in the Earth has been relatively constant throughout time, that the Moon was at 3 Earth radii (R_e) at 4.6 x 10^9 yr ago, and using the theoretical expression in which $D_e \propto t^{2/13}$, where t is the time (Turcotte *et al.*, 1977). The former assumption is not necessarily correct since the current rate of change of D_e is a factor of 4.5 times greater than that derived from the theoretical curve in Figure 1. Also growth ring data from corals, bivalves, and stromatolites indicate that the average rate of change of D_e since the Devonian has been about 3 times the theoretical value (Wells, 1963; Scrutton, 1965). However, the dissipation rate during most of geological time cannot have been as high as it has been in the last few hundred million years. If it were, the Moon would have been at $3R_e$ only about 2 x 10^9 yr ago, and this is excluded on a number of grounds. Also, because of the $D_e^{13/2}$ dependency of the time-scale, it is unlikely that the actual variation of D_e with time deviated too widely from the theoretical curve during lunar history. As such, the $D_e(t)$ curve tied to the stromatolite point in Figure 1 is a conservative estimate of the lower limit for $D_e(t)$. Using the two curves in Figure 1 to define limiting

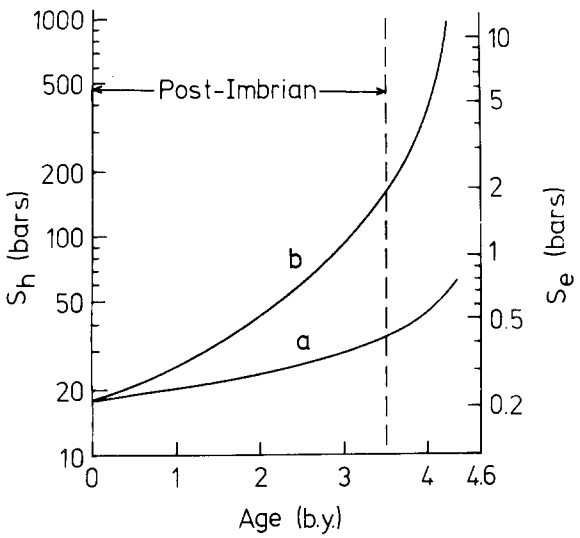

Fig. 2. Stress in the crust for a hydrostatic lunar model with a thin crust (S_h) and for an elastic, but incompressible lunar model (S_e) caused by changes in the tidal and rotational figure of the Moon as functions of time. Curves *a* and *b* are based on curves D_e(theory) and D_e(minimum) in Figure 1, respectively. See text for details.

$D_e(t)$'s and (4) and (5), one obtains σ_t (Figure 2) as functions of time for the hydrostatic and elastic Moon models.

From Figure 2 one can see that the maximum stress produced in the thin crust of a hydrostatic Moon as its figure relaxed from the form it had at the beginning of the post-Imbrian to its current figure is 18 bars for the most probable $D_e(t)$ and 140 bars for the most conservative $D_e(t)$. These values represent the upper limits for the stress produced by change of figure effects in the crust during the post-Imbrian. The lower limits for these stresses are found using the elastic, but incompressible model. In this case the maximum stress is 0.3 bars and 2.3 bars for the probable and conservative $D_e(t)$'s, respectively. Since the real Moon lies somewhere within these limits, it is clear that the maximum stress caused in the crust by post-Imbrian tidal and rotational effects is only on the order of a few ten's of bars or less. As seen by comparing these results with those given in the following sections, stresses in this range are at least two orders of magnitude smaller than those needed to produce faulting. Hence the tidal and rotational stresses are not a significant source – or even an influencing factor in controlling the pattern of post-Imbrian tectonism.

2.2. Minimum Thermoelastic Stress Models

Solomon and Chaiken (1976) and Solomon and Head (1979) have presented models of the stress history of a Moon with an initial temperature profile due to accretional heating. Such models have cool (~ 300 °C) deep interiors and outer molten zones only a few (~ 300 km) hundred km deep (see Figure 1 of Solomon and Chaiken, 1976). These

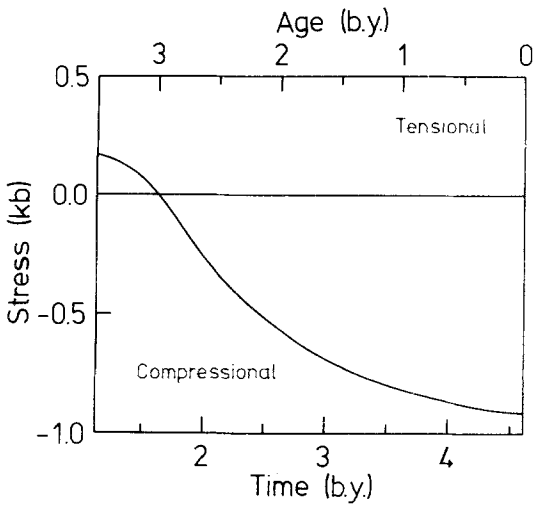

Fig. 3. Compressional thermoelastic stresses in the outer crust as a function of time according to the models of Solomon and Chaiken (1976) and Solomon and Head (1979). The figure is adopted from Figure 11 of Solomon and Head.

models were specifically developed to have a thermally induced decrease of the radius of $\lesssim 1$ km and compressional tangential stresses (σ_{ct}) in the crust of only hundreds of bars during lunar history. These constraints were used since there are no large scale thrust faults on the lunar surface and Solomon and Chaiken argued that such faults should exist if the compressional stresses were more than about 500 bars. This stress limit was increased to nearly 1 kbar in the model presented by Solomon and Head (1979); however, the basic arguments used are the same for both models. In either case, these types of models have low values of σ_{ct} in the crust during the post-Imbrian and are representative of all such accretional heating models. The integrated compressional stress at the lunar surface as a function of time for the Solomon and Head (1979) model is given in Figure 3.

2.3. High Thermoelastic Stress Model

Binder and Lange (1980) have presented a model of the stress history of a fissioned Moon which was initially totally molten. These authors show that the empirical basis for the $\lesssim 1$ km for the decrease in the radius (ΔR) of the Moon during its history was incorrectly interpreted by Solomon and Chaiken (1976) and that a conservative analytical treatment of thrust fault mechanics (Anderson, 1951) indicates that compressional tangential stresses of at least 1 to 2 kbar are needed to produce thrust faulting in the outer crust. Hence the $\Delta R \lesssim 1$ km and $\sigma_{ct} < 1$ kbar limits of Solomon and Chaiken were not used as constraints in the Binder and Lange modeling. Their model has ΔR of 5.4 km and stresses in the outer crust of up to 3.5 kbar. The stresses in the lunar crust during the post-Imbrian as derived from Figure 6 of Binder and Lange (1980) are given here in Figure 4 as functions of depth and time.

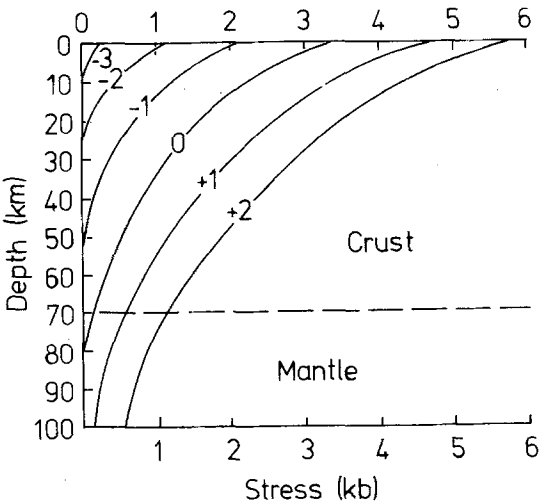

Fig. 4. Compressional thermoelastic stresses in the outer part of the Moon as functions of time and depth in the Moon according to the model of Binder and Lange (1980). Curve 0 gives the stresses at the present. Curves − 1, − 2, and − 3 give the stresses at 1, 2, and 3 billion years in the past. Curves + 1 and + 2 gives the stresses at 1 and 2 billion years in the future.

3. Thrust Fault Dynamics

As reviewed by Binder and Lange (1980; see their Equations 10–14) fault dynamics theory (Anderson, 1951) shows that σ_{ct} needed to produce thrust faulting (the only type possible due to global stresses during the post-Imbrian, see the discussion by Binder and Lange) is given by

$$\sigma_{ct} \geqslant K\rho g z + S, \tag{7}$$

where ρ is the density of crustal rocks ($\sim 2.9\ \mathrm{gm\ cm^{-3}}$), g is the gravity ($162.3\ \mathrm{cm\ s^{-2}}$), z is the depth to the fault surface, S is the average crushing strength of lunar rocks (~ 4 kbar, Mizutani *et al.*, 1977), and K is a function of the coefficient of friction (F), defined by

$$K = \frac{\sqrt{1+F^2}+F}{\sqrt{1+F^2}-F}; \tag{8}$$

while the angle (θ) between the maximum stress vector and the fault plane is given by

$$\theta = (1/2)\ \mathrm{arc\ tan}\ (1/F). \tag{9}$$

For terrestrial faults, F lies between 0.75 and 1.5 (Anderson, 1951; Sibson, 1974). Binder and Lange used $F = 0.75$ in their discussion of lunar faulting, and hence θ is about 26° in their model. However, it is likely that F for the Moon is near the upper end of the terrestrial range due to the anhydrous nature and low volatile content of the lunar rocks. On the basis of these considerations, and since none of the major conclusions presented in

this paper are critically dependent on the exact value of F used in the model (see footnote in Table II), it is assumed for simplicity in the following that $F \sim 1.5$ may be typical for the Moon and hence by (8) $K \sim 11$ in (7).

Also as part of their assessment of lunar faulting, Binder and Lange assumed that S in (7) is zero in the outer several (~ 10) km of the crust and that S reaches its full average value of about 4 kbar at about 20 km depth (see their Figure 7). They argued that pre-existing fault planes might be open in the brecciated outer zone of the crust. Thus σ_{ct} would not have to overcome the breaking strength (S) of the rocks in order to initiate fault movement. However, this conservative assumption is unlikely. As discussed by Binder and Lange, their thermoelastic stress model and those of Solomon and Chaiken (1976) show that the global stresses prior to 3.5×10^9 yr ago were tensional in the crust. Hence these stresses would have produced only normal faults during the first quarter of lunar history. Also the faulting associated with the mare basins – i.e., the concentric scarps and the radial lineaments, are clearly expressions of normal faulting. Finally, there does not seem to be any references to old thrust fault scarps in the literature. Thus it appears that normal faulting dominated Imbrian and pre-Imbrian tectonism. Therefore pre-existing thrust fault planes *do not exist*. While post-Imbrian thrust faulting could reactivate old thrust faults, this is *not* the case for old normal faults. Equation (9) is valid for both normal and thrust faults, the principle stress vector being vertical for the former and horizontal for the latter. Thus the dip angle for normal faults ($F = 1.5$ as above) should be typically 73° and that for the thrust faults is 17° as given earlier. This 54° difference in the fault plane dips makes it impossible for thrust faults to reactivate old normal faults. The tangential stresses required to shove a thrust block up a 73° inclined old fault plane can easily be shown to be infinitely greater than the crushing strength of the rocks. Hence the stresses will cause a new fault plane to develop with the appropriate dip (17°) long before they can reactivate an old normal fault plane.

It is, nevertheless, possible that $\bar{S}$ is considerably less than 4 kbar in the breccia zone of the upper crust. However the outcrops observed by the Apollo 15 astronauts on the wall of Hadley Rille indicate that relatively competent rock is found immediately below the regolith at this mare site. As shown here in Table I and in Figure 6 of Horvath *et al.* (1980), the P and S wave structure of at least the outer 150 m of the crust is very similar at *all mare* and *highland sites* where measurements were made. Thus since the P wave velocities in the layers immediately under the regolith at the 12, 14, 16, and 17 sites are equal to or greater than that at the 15 site, rocks about as competent as those observed by the astronauts at 15 must also lie under the regolith at the other four sites. Further, the seismic data indicate that the P and S wave velocities reach those of competent rock at all sites within the first kilometer of the surface (Cooper *et al.*, 1974; Koyama and Nakamura, 1979). Thus it appears that the effects of brecciation on the strength of lunar rocks is about the same for both the highlands and the maria and is not significant at depths below 1 km and may not be too important ($<$ factor 10) even at very shallow depths (10's of meters). As such, S in (7) is taken as the full crushing strength of the rocks at all depths in the crust.

TABLE I

P-wave velocities in the outer crust

	Apollo landing site				
Layer	12[a]	14[b]	15[a]	16[b]	17[b]
Regolith					
max. depth	$\simeq$ 3.7 m	8.5 m	$\simeq$ 4.4 m	12.2 m	~ 4 m
Vp	95 m s^{-1}	104 m s^{-1}	98 m s^{-1}	114 m s^{-1}	~ 100 m s^{-1}
2nd					
max. depth	?	> 27–84 m	?	> 80 m ?	32 m
Vp	$\simeq$ 245 m s^{-1}	299 m s^{-1}	$\simeq$ 255 m s^{-1}	250 m s^{-1}	327 m s^{-1}
3rd					
max. depth	–	–	–	–	390 m
Vp	–	> 386 m s^{-1}	–	–	495 m s^{-1}
4th					
max. depth	–	–	–	–	1380 m
Vp	–	–	–	–	960 m s^{-1}
5th					
max. depth	–	–	–	–	?
Vp	–	–	–	–	> 4700 m s^{-1}

[a] Nakamura *et al.*, 1975.
[b] Cooper *et al.*, 1974.

According to Table 16.1 of Howell (1959) the crushing strength of terrestrial igneous rocks ranges from about 500 bars to about 3.5 kbar and average about 2 kbar. Mizutani *et al.* (1977) have shown that the crushing strength of rocks under lunar conditions (vacuum and no volatiles) rises by a factor of two, i.e., $\bar{S}$ is about 4 kbar. Hence the expected range of S for lunar rocks should be 1 to 7 kbar. This conclusion and that given above regarding the coefficient of friction of lunar materials (i.e., $F \cong 1.5$) leads to (7) which in the case of the Moon assumes the values of

$$\sigma_{ct} \geqslant 11\rho gz + (4 \pm 3)\,\text{kbar} \tag{10}$$

or

$$\sigma_{ct} \geqslant 0.51z\ \text{kbar/km} + (4 \pm 3)\,\text{kbar}. \tag{11}$$

4. Post-Imbrian Global Tectonism

From the discussion given above, post-Imbrian global tectonism is expected to be limited to thrust faulting (and possibly folding, not discussed here) caused by thermoelastic stresses and described by (11). Figure 5 is a summary diagram containing the stress model data given in Figures 3 and 4 and the minimum σ_{ct} needed to initiate thrust faulting. From Figure 5 it is clear that the minimum thermoelastic stress models of Solomon and Chaiken (1976) and Solomon and Head (1979) have stresses which are too low to produce any global thrust faulting.

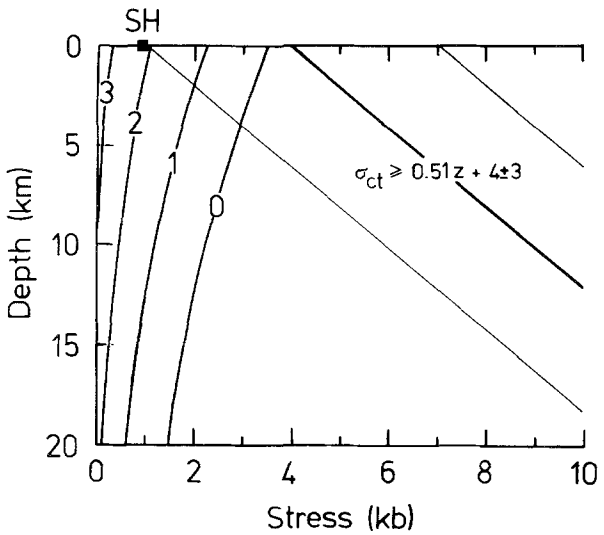

Fig. 5. Tectonic parameters in the outer 20 km of the crust. The filled square labeled SH is the maximum compressional stress in the crust as taken from the Solomon and Head (1979) model, see Figure 3. Curves 0, 1, 2, and 3 are the stresses at present, and at 1, 2, and 3 billion years ago, respectively, according to the Binder and Lange (1980) model. The heavy straight line and the two light, parallel lines give the average, maximum, and minimum stresses needed to initiate thrust faulting in the lunar crust according to (11), i.e., $\sigma_{ct} \geq 0.51z$ kbar km^{-1} + (4 ± 3) kbar.

In contrast, Figure 6 shows that the high stress model of Binder and Lange (1980) indicates that thrust faulting can occur at present in the outer 4 km of the crust in response to stresses in the 3 to 3.5 kbar range. It seems likely that such faults would not be very large, since (1) σ_{ct} has not yet reached the average crushing strength of the rocks and thus the faults are limited to those areas where the rocks are the weakest and (2) it seems likely, based on geometric considerations, that the horizontal dimensions of the individual fault planes should be only a few times their vertical dimensions, i.e., 10 km scale. This epoch of thrust faulting may have begun between 1.5 and 2 x 10^9 yr ago as the stresses reached the crushing strength of the weakest rocks (~ 1 kbar) in the outer few hundreds of meters to 1 km of the crust. However, by the arguments given directly above, these early faults should have been very small and few in number. Thus significant faulting probably only began when the stresses reached the 2 to 3 kbar range, i.e., the faulting epoch is only 0.5 to 1 x 10^9 yr old. During this time the level of tectonic activity steadily increased and it will continue to do so during the next 3 x 10^9 yr. At that time the stresses will finally have reached the upper limit of S (~ 7 kbars) at the surface and faulting will occur to a depth of about 10 km. After 3 x 10^9 yr the level of activity may begin to slowly fall off as the zone of new fault plane formation moves deeper into the crust. Thus the Moon may have moved into a long lasting epoch of surface and crustal deformation during the last quarter of its history. Interestingly, this model indicates that the Moon is not tectonically dead, rather it is *now* beginning to be increasingly tectonically

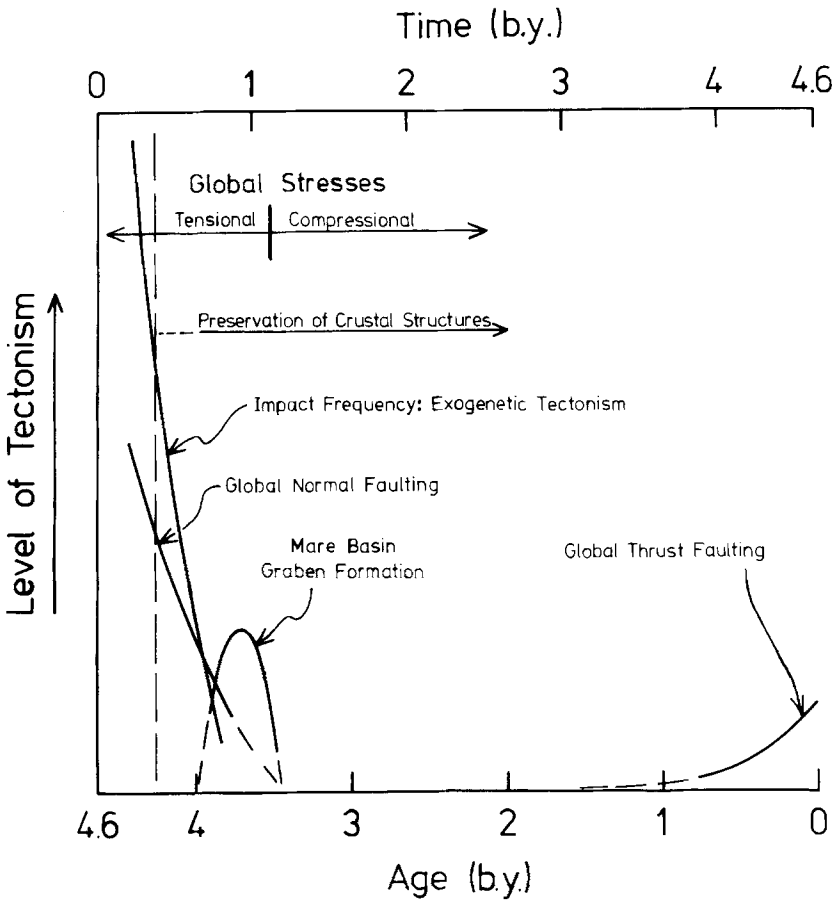

Fig. 6. Tectonic history of the Moon, based in part on the thermoelastic stress model of Binder and Lange (1980). See text for details.

active after a 2 billion year period of inactivity! Figure 6 gives a schematic representation of the global tectonism during lunar history based on this model.

Thus according to the minimum stress model the post-Imbrian should have been free from global tectonic activity and the crust should be seismically quiet on the global scale. In contrast the high stress model indicates that there should be young ($\lesssim 0.5$ to 1×10^9 yr old) thrust fault scarps of modest size (10 km scale) found on the surface and that high stress (up to ~ 3 kbar) compressional moonquakes should be occurring in the outer few (<4) km of the crust. The high stress, initially totally molten Moon model is favored by the available data.

4.1. SELENOLOGICAL EVIDENCE

Since the post-Imbrian tectonism of the maria is a product of both regional and global stresses (Solomon and Head, 1979), while the post-Imbrian tectonism of the highlands is due only to the global stresses, as discussed above, the latter offer the best place to look

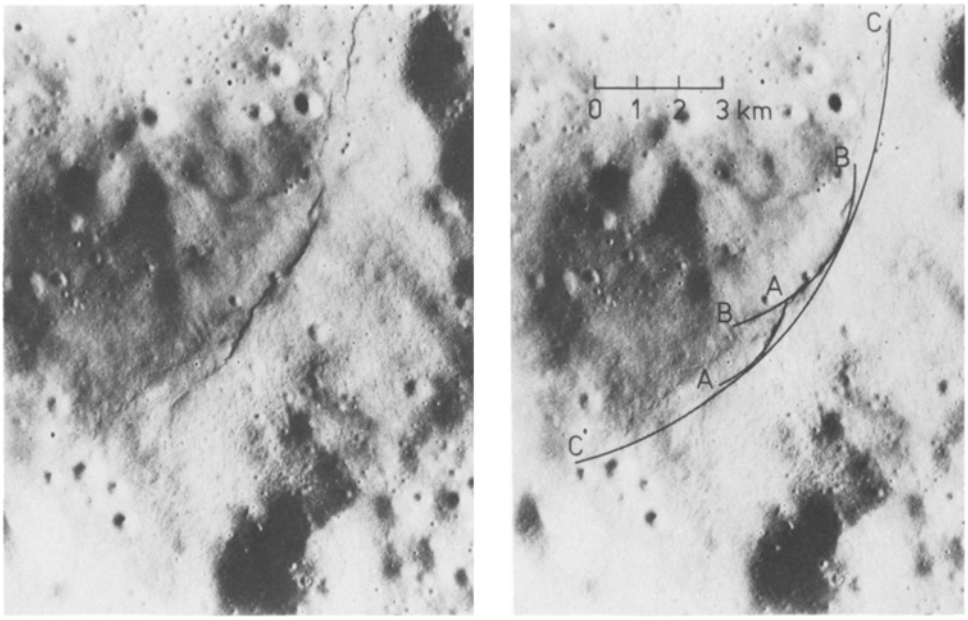

Fig. 7. Highland scarp near Mendeleev. See text for details. The photo on the right identifies the arcuate scarp segments listed in Table II.

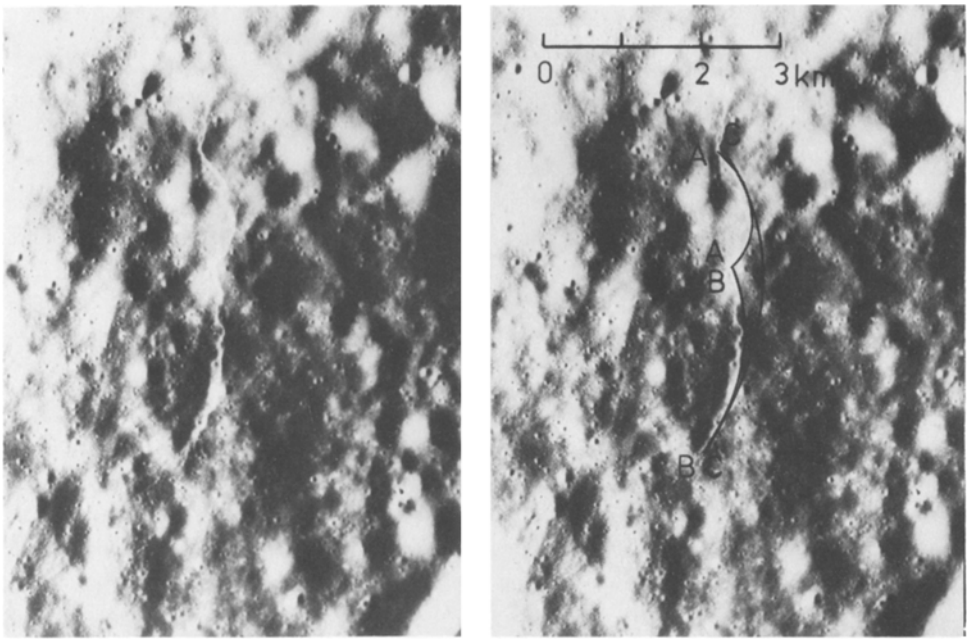

Fig. 8. Highland scarp on the floor of Mandel'shtam. See text for details. The photo on the right identifies the arcuate scarp segments listed in Table II.

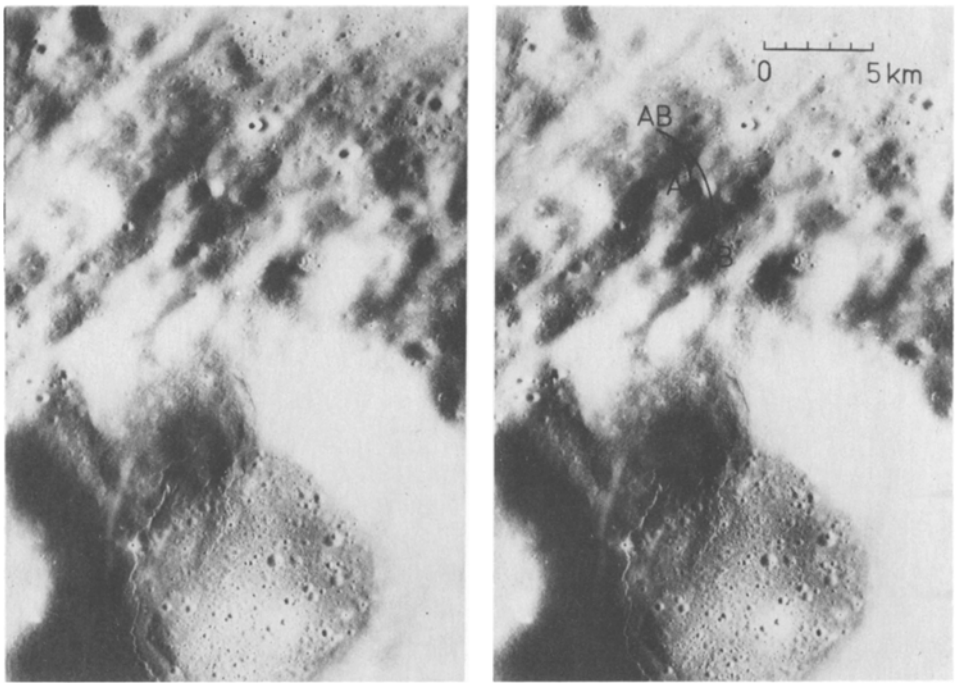

Fig. 9. Highland scarps near Atkin. Note that the scarp in the intercrater area faces east, while those occurring near the contact between the crater wall and the impact melt unit face west. See text for details. The photo on the right identifies the arcuate scarp segments listed in Table II.

for the young, small thrust fault scarps predicted by the high-stress model. A cursory review of high resolution Apollo imagry (e.g., Masursky *et al.*, 1978) shows that small scarps with the expected characteristics are found throughout the highlands. Figures 7–9 show examples of such scarps. In the caption describing Figure 87 of Masursky *et al.* (here Figure 7), Hodges writes that 'Small scarps of this kind – unrelated to any apparent source material or to any detectable tectonic control – are widely scattered in the highlands; their origin remains enigmatic'. In describing such '. . . typical far-side highlands . . .' scarps as observed by the Apollo 16 astronauts and in reference to their Figure 28-6 (here Figure 8), Mattingly *et al.* (1972) note that 'The fine scarps have the appearance of "flow fronts", yet they lack evidence of source or of surface flow patterns', and that 'A perplexing phenomenon was that when tracing an apparent west-facing scarp it would suddenly become an east-facing scarp', e.g., see Figure 9. The size, lack of apparent tectonic control, and the reversal of the direction of the scarp fronts are consistent with the concept that these features are the surface expressions of the predicted, small thrust falults formed in a relatively isotropic crust undergoing isotropic tangential compression.

An estimate of the ages of these scarps can be made on the basis of the morphologies of the craters which are partially overrun by the fault fronts or which are cut by the fault surfaces. An excellent example of the latter type crater is found near the center of scarp

B in Figure 7. This 250 m crater and several smaller craters (visible on the original photographs with diameters as small as 40 m). which are situated along the scarp fronts shown in Figures 7–9, belong to Trask's (1971) class 2, class 3, and possibly class 4 craters. According to the calibration data of Moore *et al.* (1980) the ages of the observed craters range from $7 \pm 4 \times 10^7$ to $5 \pm 2 \times 10^8$ yr (with an absolute uncertainty of a factor of ± 3). From these crater ages, it is clear that the faults which cut these craters formed only during the last few $\times 10^8$ yr, i.e., exactly the period expected if these scarps are the surface expressions of the predicted thrust faulting.

A characteristic of some of these small highland scarps is that they are at – or follow the contact between an impact melt unit in the bottom of a crater and the crater wall (Figure 9). As seen in Figure 9, it also appears that the scarps along these contacts are more fully developed than the scarps in the inter-crater areas. These observations may be explained as follows; (1) The dip of the contact between the bottom of the impact melt unit and the original crater wall must be close to the 17° dip required for thrust faulting. This is the case since the wall slope at the contact is equal to or less than the average wall slope, which for craters of the appropriate size range and morphology is 20° to 26° (Wood and Anderson, 1978). (2) These contacts most certainly are also zones of weakness. Thus these two effects may lead to the development of a thrust plane along such a contact at relatively low stresses ($\lesssim 1$ kbar). Such contact faults would therefore develop earlier than the faults in the more competent inter-crater rocks. Hence the scarps along the contacts would be the oldest and have the largest displacements.

A characteristic of the apparently more frequent inter-crater scarps is that they consist of a series of arcuate segments with the smaller segments having the smallest radius of curvature. The smaller segments tend to be near the center of – and are the best developed parts of the larger composite arcuate scarps (see especially Figure 7). This geometry suggests that the thrust fault surfaces are segements of right angle cones, rather than being planar. This suggestion is supported by the results of Jacobs *et al.* (1959) who show that such conical fault planes are the expected form in an isotropic, tangential stress field. If this is the case, then the faulting is analogous to conchoidal fracturing in obsidian, and the polar equation for the fault surface is of the form

$$z = r \tan \theta \tag{12}$$

in the coordinate system depicted in Figure 10a. Since θ is the dip angle (17°) and r is the radius of curvature of the scarp, the depth (z) to the apex of the conical segment can easily be determined. Note that z is clearly the maximum depth to which the faulting occurred for the scarp in question. This being the case then as σ_{ct} increased with time, as in Figure 5 or 6, and hence z could increase, r would also increase. Thus the smaller the radius of curvature of an arcuate segment, the older the segment and the shallower the depth of faulting which caused it. As σ_{ct} and z increased, the small segments would coalesce to form a larger scarp. The ideal situation is that the centers of the every larger cones would lie on a straight line as shown in Figure 10b, but the more likely situation is shown in Figure 10c.

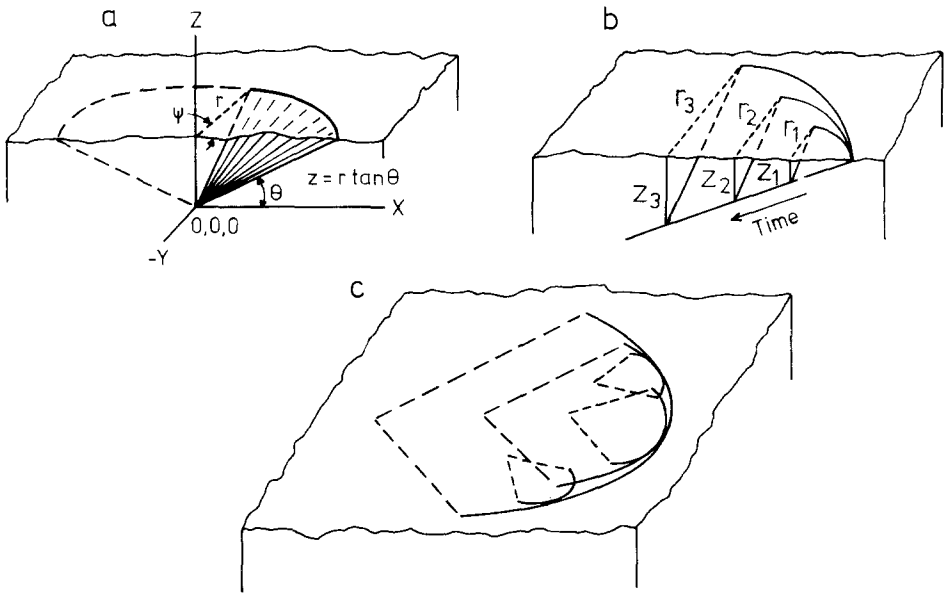

Fig. 10. Apparent geometry of the highland thrust scarps. As is shown in Section a, the thrust fault surface (the lineated surface) is a segment of a right angle cone whose apex is at 0, 0, 0. The lunar surface is parallel to the x, y plane and is at z distance from the origin. The fault scarp has a radius r and a half angle of Ψ at the surface. θ is the dip angle of the fault surface. Section b shows the ideal development of a compound scarp as the stresses increase with time and hence the depth of faulting, z, and the radius of the segments, r, also increase. In the ideal case the centers of the ever larger cones might lie on a straight line. Section (c) shows the more likely geometry of a composite scarp system. See text for further details.

Table II gives the data obtained for 9 arcuate scarps or scarp segments found in the inter-crater plains of Figures 7–9. The data given in the first column for z are computed by (12) assuming that θ is 17°. The second column gives the half angle (Ψ) of the segment (Figure 10a). It was noticed that Ψ does not vary very much and that $\bar{\Psi}/2$ is essentially identical to 17°. These observations suggest that there might be a physical relationship between the dip and the half angle of the scarp. It was therefore *tentatively* assumed that

$$\theta = \Psi/2. \tag{13}$$

On the basis of this assumption, r and Ψ were used as the observables and (13), (12), and (9) were used to derive θ', z', and F, respectively, as given in Table II.

The results given in Table II show several interesting points. First is the above mentioned small range of Ψ and the possible dependence of Ψ on θ. Whether or not the proposed constant of proportionality in (13) is 1/2 cannot be determined without independent measurements of θ for a large number of highland scarps. However, if there is a physical relationship between θ and Ψ and the proportionality constant is 1/2, then the results indicate that F is very close to 1.5 and θ is very close to 17°. Second, the depths of faulting, using either z or z', are all less than the maximum of 4 km derived from (11)

TABLE II

Thrust fault data

Scarp [a]	z [b]	Ψ	θ'	z'	F
7 A	680 m	27.4°	13.7°	540 m	1.93
7 B	930 m	42.4°	21.2°	1180 m	1.10
7 C	3250 m	37.2°	18.6°	3570 m	1.32
8 A	250 m	49.4°	24.7°	370 m	0.86
8 B	750 m	27.2°	13.6°	590 m	1.95
8 C	990 m	33.0°	16.5°	960 m	1.54
9 A	810 m	32.0°	16.0°	760 m	1.60
9 B	2360 m	27.0°	13.5°	1850 m	1.96
avg.	1250 m	34.4°	17.2°	1230 m	1.53
σ	± 360 m	± 2.9°	± 1.4°	± 370 m	± 0.15
δ	± 1010 m	± 8.1°	± 4.1°	± 1050 m	± 0.41

[a] Figure number and scarp identification letter.

[b] Assumes $\theta = 17°$; from Figure 5 the maximum depth of faulting is 4 km. If θ were assumed to be 26° ($F = 0.75$) as in Binder and Lange (1980), the computed depths would be 1.6 × greater than those given. However, via Figure 7 of Binder and Lange, the maximum depth of faulting would be 8 km in this case. Thus, the computed depths of faulting are less than the maximum values determined from the stress model and fault dynamics for a given value of F and the corresponding value of θ. σ, one standard deviation; δ, root mean square deviation.

and shown in Figure 5. While the largest fault reaches a depth of 3.2–3.6 km, the average depth of faulting is about 1250 m, and the mode depth is only about 730 m. Thus these results are consistent with (1) the fault dynamic model presented, (11), (2) the concept that σ_{ct} must be in the 2 to 3 kbar range before significant thrust faulting can occur in the lunar crust, and (3) the proposal that these scarps are due to thrust faulting as predicted by the high stress, initially totally molten model of Binder and Lange (1980). Clearly, the evidence provided by this cursory look at the selenological data are insufficient to demonstrate the validity of the models. However, the results are very suggestive. As such a full scale photoselenological program has begun in order to more fully characterize these features and to determine if, as seems likely, they are the predicted thrust fault scarps.

4.2. SELENOPHYSICAL CONSIDERATIONS

The HFT moonquakes have been regarded as being true tectonic quakes since their discovery (Nakamura *et al.*, 1974). Nakamura *et al.* (1979) have shown that the majority, but not necessarily all of the HFT's occur in the upper mantle at depths between the crust-mantle boundary and 200 km. However, Goins (1978) has shown that the inversion of travel time data for eight of the largest and best observed HFT's have the smallest variance when the events are assumed to have occurred at or near the surface – i.e., the largest HFT's are near surface events.

Binder and Lange (1980) have shown that tensional moonquakes with stress drops of about 200 bars are expected to occur at depths between 80 and 200 km in the mantle on the basis of their thermal history – stress history model. Their model also shows that

compressional moonquakes with stress drops of ~ 1 to 3 kbar are expected to occur at depths between 0 and 10 km in the crust. (On the basis of the nonconservative evaluation of the constants in (7) given in this paper, the depths of occurrence and the stress drops of the compressional quakes is 0 to 4 km and ~ 1 to 3 kbar, respectively.) Binder and Lange identify HFT's with (1) their model tensional moonquakes in the mantle and (2) their model compressional quakes in the upper crust (here 4 km) just below the seismic scattering zone (outer few (1–3?) km of the crust) – i.e., there are theoretically two types of HFT moonquakes. Binder and Lange further point out that those compressional moonquakes which their model predicts should occur *in* the scattering zone of the outer few km of the crust would *not* be identified as HFT's. Thus there should be a third, but as yet unidentified class of moonquakes which occur in the outer 1 to 3 km of the crust. These quakes are genetically the same as the compressional HFT's occurring at 4 km depths, but are, as yet, indistinguishable from impact events. It is proposed here that the shallow compressional moonquakes (large HFT's and as yet unidentified) are the seismic expressions of the post-Imbrian thrust fault tectonism discussed in this paper. If so, then these quakes accompany the formation and further development of the 10 km scale highland scarps discussed in this paper and the mare ridges. Unfortunately, the small number of observed HFT's (~ 30) and the relatively large uncertainty in the determinations of their epicenters and focal depths do not yet allow photo-selenological and seismological observations to test this conclusion.

5. Summary

Evaluation of all reasonable sources of stress in the lunar crust indicates that compressional thermoelastic stresses are the only ones which have been tectonically significant on the global scale during the last 3.5×10^9 yr of lunar history (i.e., the post-Imbrian). However, the thermoelastic stresses calculated for lunar models which have accretional heating profiles at the beginning of lunar history – i.e., a molten zone only a few hundred kilometers deep and a cool interior – are lower than those required to initiate thrust faulting in the crust. Thus such models predict that no significant global thrust faulting has occurred during the post-Imbrian and that the crust should be currently seismically quiet on the global scale.

In contrast, the compressional thermoelastic stresses generated in a Moon which was initially totally molten are up to 3.5 kbar in the outer few km of the crust at present. These stresses are well within the range needed to cause significant thrust faulting in the outer 4 km of the crust. According to this model there should be modest scale (10 km), young ($\leqslant 0.5$ to 1×10^9 yr old) thrust fault scarps in the highlands. Also shallow, compressional moonquakes (HFT's and a genetically identical, but as yet unidentified type) with stress drops in the 3 kbar range should be occurring on these thrust faults.

Photoselenological investigations confirm that scarps with the expected age and geometric characteristics are found scattered in the highlands. Thus, the currently available photoselenological data support the stress model derived for an initially totally molten

Moon, but not one which was molten only in the outer few hundreds of km. As such the results presented here support the binary fission model for the origin of the Moon (e.g., Binder, 1974, 1978, 1980) or those models in which the Moon formed by accretion, but underwent very rapid ($\lesssim 10^7$ yr) total melting (Runcorn, 1977).

Acknowledgement

This work was supported by the Deutsche Forschungsgemeinschaft.

References

Anderson, E. M.: 1951, *The Dynamics of Faulting*. Oliver and Boyd, Edinburgh.
Binder, A. B.: 1974, *Moon* **11**, 53.
Binder, A. B.: 1978, *Earth Planet. Sci. Lett.* **41**, 381.
Binder, A. B.: 1980, *Proc. Lunar Planet. Sci. Conf. 11th*, 1931.
Binder, A. B. and Lange, M. A.: 1980, *J. Geophys. Res.* **85**, 3194.
Comer, R. P., Solomon, S. C., and Head, J. W.: 1979, *Proc. Lunar Planet. Sci. Conf. 10th*, 2441.
Cooper, M. R., Kovack, R. L., and Watkins, J. S.: 1974, *Rev. Geophys. Space Phys.* **12**, 291.
Goins, N. R.: 1978, *The Internal Structure of the Moon*. PhD thesis, MIT, Cambridge.
Horvath, P., Latham, G. V., Nakamura, Y., and Dorman, H. J.: 1980, *J. Geophys. Res.* **85**, 6572.
Howell, B. F., Jr.: 1959, *Introduction to Geophysics*, McGraw-Hill, New York.
Jacobs, J. A., Russell, R. D., and Wilson, J. T.: 1959, *Physics and Geology*, McGraw-Hill, New York.
Jeffreys, H.: 1962, *The Earth*. University Press, Cambridge.
Koyama, J. and Nakamura, Y.: 1979, in *Lunar and Planetary Science X*, 685, Lunar and Planetary Institute, Houston.
Longhi, J.: 1977, *Proc. Lunar Sci. Conf. 8th*, 601.
Masursky, H., Colten, G. W., and El-Baz, F.: 1978, *Apollo over the Moon: A View from Orbit*. NASA, Washington, D.C.
Mattingly, T. K., El-Baz, F., and Laidley, R. A.: 1972, in *Apollo 16 Preliminary Science Report*, 28-1, NASA, Washington, D.C.
Melosh, H. J.: 1977, *Icarus* **31**, 221.
Melosh, H. J.: 1980, *Icarus* **43**, 334.
Mitzutani, H., Spetzler, H., Getting, I., Martin III, R. J., and Soga, N.: 1977, *Proc. Lunar Sci. Conf. 8th*, 1235.
Moore, H. J., Boyce, J. M., and Hahn, D. A.: 1980, *Moon and Planets* **23**, 231.
Nakamura, Y., Dorman, J., Duennebier, F., Ewing, M., Lammlein, D., and Latham, G.: 1974, *Proc. Lunar Sci. Conf. 5th*, 2883.
Nakamura, Y., Latham, G. V., Dorman, H. J., Ibrahim, A. K., Koyama, J., and Horvath, P.: 1979, *Proc. Lunar Planet. Sci. Conf. 10th*, 2299.
Nakamura, Y., Dorman, J., Duennebier, F., Lammlein, D., and Latham, G.: 1975, *The Moon* **13**, 57.
Runcorn, S. K.: 1977, *Proc. Lunar Sci. Conf. 8th*, 463.
Scrutton, C. T.: 1965, *Paleontology* **7**, 552.
Sibson, R. H.: 1974, *Nature* **249**, 542.
Solomon, S. C. and Chaiken, J.: 1976, *Proc. Lunar Sci. Conf. 7th*, 3229.
Solomon, S. C. and Longhi, J.: 1977, *Proc. Lunar Sci. Conf. 8th*, 583.
Solomon, S. C. and Head, J. W.: 1979, *J. Geophys. Res.* **84**, 1667.
Trask, N. J.: 1971, *U.S. Geol. Survey Prof. Paper 750D*, D138.
Turcotte, D. L., Cisne, J. L., and Nordmann, J. C.: 1977, *Icarus* **30**, 254.
Wells, J. W.: 1963, *Nature* **197**, 948.
Wood, C. A. and Anderson, L.: 1978, *Proc. Lunar Planet. Sci. Conf. 9th*, 3669.